A Comparative Study of Anti-Jamming Beamforming Using Deep Learning in Planar Phased Array Antennas

Aymen Alhamdan[1], Lotfi Laadhar[1], Mohammed Aseeri[2*], Abdullah Dobaie[1], and Hatem Rmili[1]

[1]Faculty of Engineering, Electrical and Computer Engineering Department
King Abdulaziz University, P.O. Box 80204, Jeddah 21589, Saudi Arabia
Aalhamdan0025@stu.kau.edu.sa, lladhar@kau.edu.sa,
adobaie@kau.edu.sa, hatem.rmili@kau.edu.sa

[2]Next Generation Connectivity and Wireless Sensors Institute
King Abdulaziz City of Science and Technology (KACST), Riyadh, Saudi Arabia
masseri@kacst.gov.sa
*Corresponding Author

Abstract – In this study, a deep learning-based beamforming comparative study for anti-jamming applications in 2D-planar phased arrays is presented. For better array architecture benchmarking, three different geometries (circular, rectangular, hexagonal) are considered. Convolutional Neural Network (CNN) is employed to translate a target radiation pattern, generated as an image, directly into the optimal antenna currents. Adaptive antenna array beamforming weights can be estimated efficiently by the deep learning-based MATLAB code according to the desired beam steering angle and the null direction of the jammer. This approach establishes a smart, non-iterative mapping that bypasses traditional optimization algorithms, reducing computation time by up to 260x. Once trained, the model delivers optimal currents and weights in a single and efficient forward pass.

Index Terms – Antenna arrays, anti-jamming, beamforming, deep learning.

I. INTRODUCTION

Active Electronically Scanned Arrays (AESA) provide rapid electronic beam steering, flexible beamshaping, and spatial filtering capabilities that are fundamental to modern radar [1–7], wireless communications [8–10], and electronic-warfare systems [11–13]. The ability to steer beams and place deep nulls enables effective target tracking and interference mitigation without mechanical motion. However, practical AESA operation depends critically on fast, reliable computation of the complex excitation coefficients for large antenna arrays. Traditional adaptive beamforming and null-steering methods (e.g., Minimum Variance Distortionless Response [MVDR], projection-based nulling, optimization-based synthesis) often involve iterative solvers or large linear-algebra operations whose runtime grows unfavorably with array size and can limit system responsiveness in highly dynamic or contested electromagnetic environments. Deep learning has emerged as a promising alternative to reduce runtime complexity by learning a direct mapping from high-level beam specifications or measured field patterns to antenna excitations [14–16]. Several recent works have shown that neural networks can produce near-optimal beamforming weights for specific array architectures or tasks (beam steering, sidelobe shaping, null placement), typically achieving large reductions in online computation time once trained [17–20]. Most deep learning studies, however, focus on a single array geometry or a narrow set of scenarios; systematic comparisons across different planar array geometries are scarce. Such comparative evaluations are important because array geometry affects beamwidth, sidelobe distribution, element coupling, and robustness to constraints-factors that influence the effectiveness of learned mappings and the practical choice of array architecture.

This paper addresses that gap by presenting a comparative study of deep learning-based anti-jamming beamforming across three planar phased-array geometries: uniform rectangular, circular, and hexagonal. We train a convolutional neural network (CNN) that accepts a desired 2D radiation-pattern image (including main-beam direction, side-lobe mask, and jammer direction) and directly predicts the complex excitation coefficients for all array elements. The image-based input encodes the target spatial specifications in a form that is geometry-agnostic, allowing a single modeling

Submitted On: January 21, 2026
Accepted On: May 04, 2026

https://doi.org/10.13052/2026.ACES.J.410401

approach to be applied to different array topologies while preserving spatial relationships in the pattern. Training reference weights are computed using the MVDR beamforming method, which provides optimal interference suppression while preserving the desired signal direction.

The key contributions of this work are:

- A unified CNN framework that translates 2D radiation-pattern images into complex excitation coefficients, enabling non-iterative beam synthesis for large planar arrays.
- A controlled comparative evaluation of three planar geometries (rectangular, circular, hexagonal) with comparable element counts, isolating the influence of geometry on deep learning prediction accuracy, beam-pointing error, sidelobe behavior, and jammer suppression.
- Comprehensive runtime and performance analysis showing that, after training, the CNN yields excitation weights with closely matching beam characteristics to conventional methods while reducing online computation time dramatically (up to $\approx 260\times$ with GPU acceleration in our experiments).
- Practical insights about geometry-dependent behaviors: the rectangular array achieved the best pattern agreement in our tests, while circular and hexagonal geometries exhibited different sidelobe placement characteristics that affected prediction fidelity.

The remainder of the paper is organized as follows. Section II details the array geometries and element placement. Section III formulates the beamforming problem and describes the CNN architecture and training procedure. Section IV presents simulation results, quantitative comparisons against conventional beamforming, runtime benchmarks, and a discussion of geometry-dependent effects. Section V concludes and outlines directions for future work.

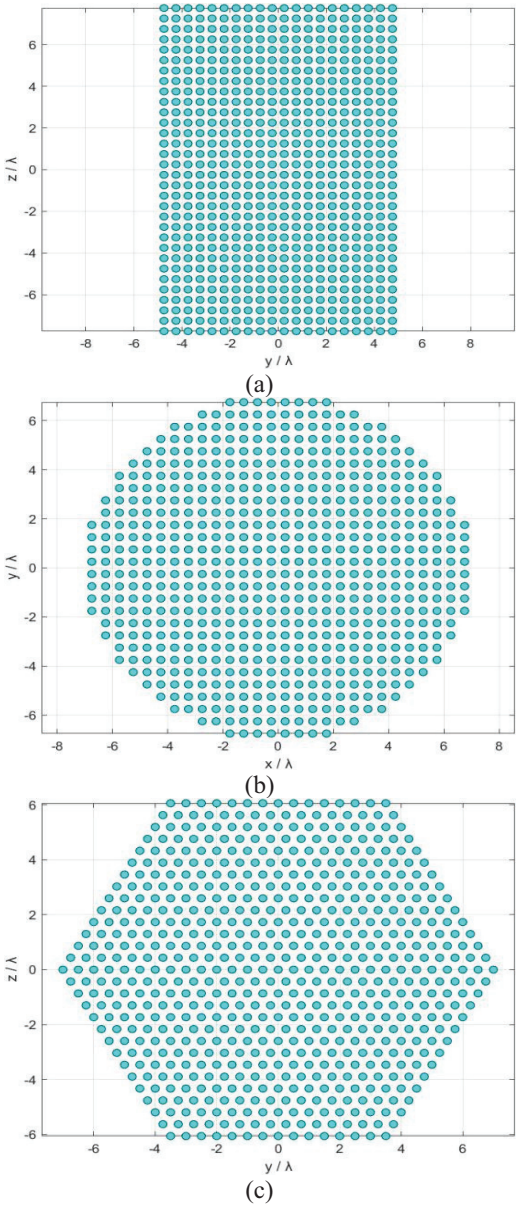

Fig. 1. Geometry of the proposed arrays: (a) rectangular array (640 elements), (b) circular array (616 elements), (c) hexagonal array (631 elements).

II. ARRAYS DESIGN

We have considered three geometries (rectangular, circular, hexagonal) of phased array antennas operating at 3.2 GHz with spacing equal to lambda by 2 (see Fig. 1). The number of elements for the rectangular, circular, and hexagonal arrays are 640, 616, and 632, respectively. We tried to select comparable number of elements for better comparison of their performance when we apply the deep learning technique. The radiating element is assumed to be an isotropic source.

The rectangular array is of length 16λ and width 10λ. The radius of the circular array and the size of each edge of the hexagonal array is 7λ, where λ is the wavelength corresponding to the operating frequency 3.2 GHz.

III. DEEP LEARNING-BASED BEAMFORMING

A. Problem formulation

We consider a rectangular planar antenna array situated in the *yz* plane where the radiating elements are separated by lambda by 2. The mathematical formulation of the problem is detailed in [21, 22]. The array

factor is given by:

$$F_A = \sum_{n=0}^{N_A-1} c_n e^{jk_0 \mathbf{k}\cdot\mathbf{r}_n}, \tag{1}$$

where $\mathbf{r}_n$ and c_n are the position vector and the complex excitation coefficient of the element n, respectively. N_A is the total number of radiating elements, k_0 is the wavenumber, and $\mathbf{k}$ is the cosine vector.

The array directivity is maximum in the direction (θ_0, ϕ_0), and is expressed by:

$$D_{\max} = K\frac{\max|F_A(\theta_0,\phi_0)|^2}{P_{\text{rad}}} = \frac{K}{P_{\text{rad}}}, \tag{2}$$

where P_{rad} is the total radiated power by the array and K is a constant. The optimization problem consists of determination of the excitation set c_i such that the total radiated power is minimum [21, 22].

In this work, we used the same procedure adopted in [15], which consists of the determination of the real and imaginary parts $(\text{Re}[c_n], \text{Im}[c_n])$ of the complex excitation coefficients c_n in the presence of four constraints: main beam direction $(\theta_{\max}, \phi_{\max})$, jammer direction (θ_j, ϕ_j), side lobe level (SLL), and required suppression level SSL_J.

B. Convolutional neural network architecture

Several CNN architectures were investigated in this work. The final architecture of the selected CNN configuration is illustrated in Fig. 2. Based on experimental evaluation, a 9-layer deep neural network was chosen, consisting of six convolutional layers followed by three fully connected layers, with the last layer serving as the output layer. The network accepts 721×721 single-channel grayscale radiation pattern images as input. Each convolutional layer employs 3×3 kernels with same zero padding. The stride is set to 1 in the first convolutional layer and 2 in the subsequent layers to progressively reduce the spatial resolution and increase the receptive field. Batch normalization and ReLU activation functions are applied after each convolutional and fully connected layer to improve training stability and convergence.

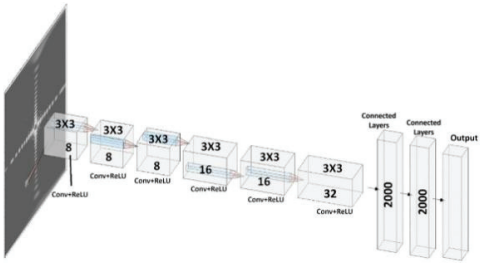

Fig. 2. Architecture of the used CNN.

The number of feature maps increases gradually from 8 to 32 across the convolutional layers, enabling hierarchical feature extraction and progressive learning of spatial features from the radiation pattern. The fully connected section consists of two hidden layers with 2000 neurons each, followed by an output layer whose size depends on the antenna geometry under consideration. Specifically, the network generates a 1280-dimensional output vector for the Uniform Rectangular Array, 1232-dimensional output vector for the Circular Planar Array, and 1262-dimensional output vector for the Hexagonal Array. Each output vector represents the concatenated real and imaginary components of the optimized antenna weights predicted by the network.

C. Training

During the training phase, we have generated 7000 radiation patterns for each phase array geometry (Rectangular, Circular, Hexagonal) corresponding to different values of $(\theta_{\max}, \phi_{\max})$, SLL, (θ_j, ϕ_j), and SLL_J. Each radiation pattern was represented as an 8-bit, single-channel grayscale image with a spatial resolution of 721×721 pixels. The simulated radiation patterns were generated using the MATLAB Phased Array System Toolbox under the following constraints.

Main lobe direction:

$$-35^\circ \le \theta_{\max} \le +35^\circ \quad \text{and} \quad -45^\circ \le \phi_{\max} \le +45^\circ,$$

Side Lobe Level:

$$\text{SLL} = -13 \text{ dB},$$

Jammer (Interference) direction:

$$-20^\circ \le \theta_j \le +20^\circ \quad \text{and} \quad -15^\circ \le \phi_j \le +15^\circ,$$

Required suppression level of SLL:

$$\text{SLL}_J = -30 \text{ dB}.$$

The generated radiation patterns were converted to decibel (dB) scale and normalized using min-max scaling to the range $[0,1]$ before being used as inputs to the CNN. The target directions were randomly sampled within the specified angular ranges to ensure dataset diversity.

The reference beamforming weights used for training were computed using the MVDR beamforming algorithm, which minimizes the array output power while maintaining a distortionless response in the desired target direction. Consequently, interference and noise are effectively suppressed, leading to significant attenuation in the jammer direction while preserving the main beam.

The complex beamforming weights were separated into real and imaginary components and normalized

prior to training to improve numerical stability. During the training process, the Adam optimizer was used with a learning rate of 0.00025, a batch size of 32, and 60 epochs. The loss function was defined as the Mean Squared Error (MSE) between the predicted weights and the corresponding reference weights.

The dataset was randomly divided into 80% for training, 10% for validation, and 10% for testing. Training, validation, and initial testing were performed on a workstation equipped with an Intel Xeon Gold 6230R processor (20 cores at 2.1 GHz), 64 GB RAM, and a single NVIDIA Quadro RTX 4500 GPU. An additional independent testing stage was conducted on a separate system using a 4-core Intel i7 processor (3.6 GHz) with 12 GB RAM.

IV. RESULTS AND DISCUSSION

For comparison, we have calculated the radiation patterns of the specified arrays under mask constraints using the conventional beamforming method MVDR (true weights) and the deep learning technique (predicted weights). We have chosen to present the results for the following case: $(\theta_{\max}, \phi_{\max}) = (0,0)$, SLL $= -13$ dB, $(\theta_j, \phi_j) = (20,15)$, and $\text{SLL}_J = -30$ dB.

These results are depicted in Fig. 3, which shows the 2D contour plot of the radiation patterns obtained using both true and predicted weights for the three arrays considered.

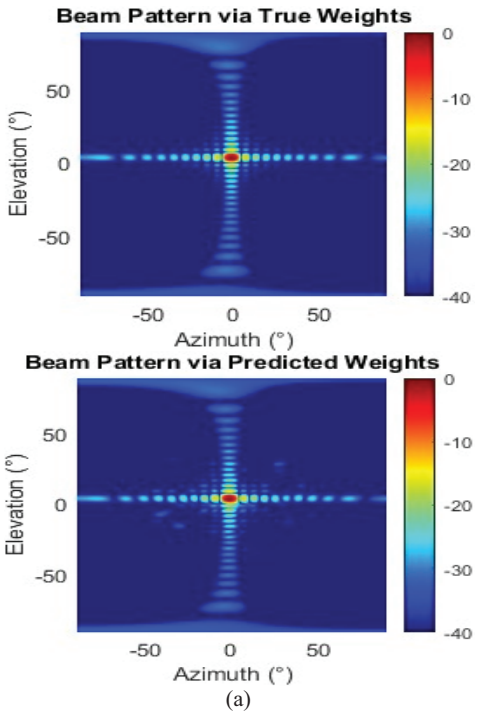

(a)

Fig. 3. Continued

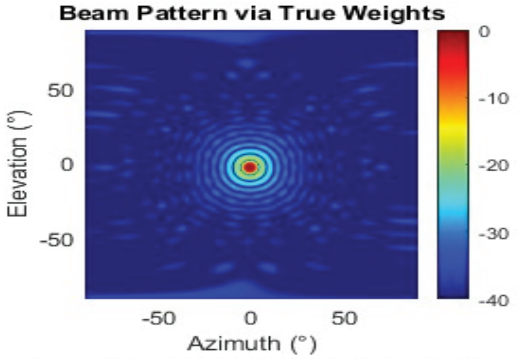

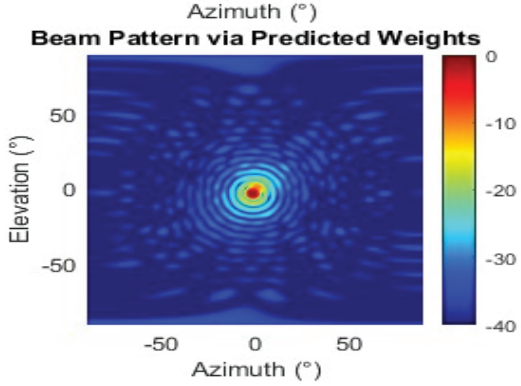

(b)

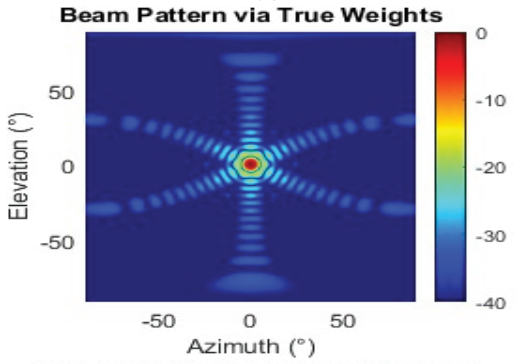

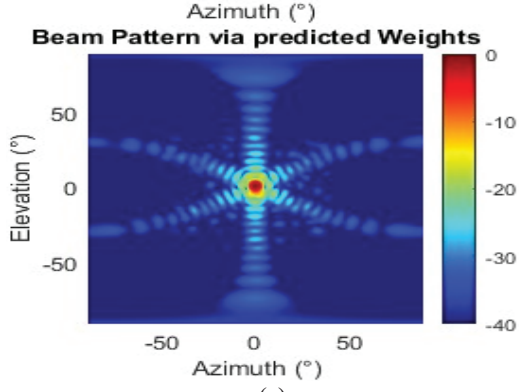

(c)

Fig. 3. 2D contour plot of the radiation patterns obtained separately with true and predicted weights (deep learning) for (a) rectangular array, (b) circular array, (c) hexagonal array.

In Fig. 3, the radiation patterns show the main lobe centered at $(0,0)$ for all the array geometries with

good agreement between patterns calculated with the true values of the excitation coefficients and the patterns determined with the predicted values by using the deep learning method. Analysis of the patterns shows that the agreement is excellent for rectangular, but less effective for circular arrays and hexagonal arrays. It is also noticeable that the secondary lobes are positioned around the main beam in the circular array, while they are distributed in various directions in the other arrays.

To enhance comparison, we have displayed the 2D radiation patterns derived from both true and predicted values in the azimuth and elevation planes, as illustrated in Fig. 4. This representation effectively highlights the alignment between conventional and deep learning beamforming techniques, as well as locating the directions of the target and the jammer within the plot.

Table 1 summarizes the key results for the three array geometries using both MVDR and the proposed deep learning method. As shown, the beam pointing error remains very small for all geometries, with deviations within a fraction of a degree, indicating accurate beam steering. The required interference suppression level is successfully achieved in all cases, with null depths exceeding −30 dB at the jammer direction. Additionally, the sidelobe levels remain within acceptable limits, confirming that the radiation pattern constraints are satisfied. The Half Power Beam Width (HPBW) values obtained using the predicted weights closely match

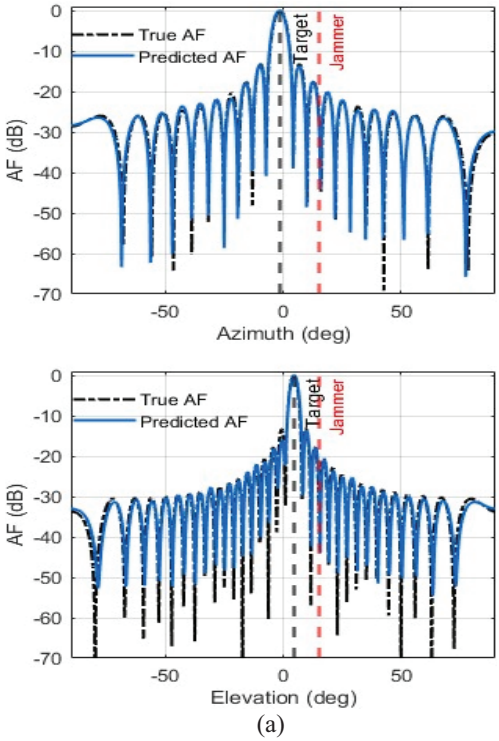

Fig. 4. Continued

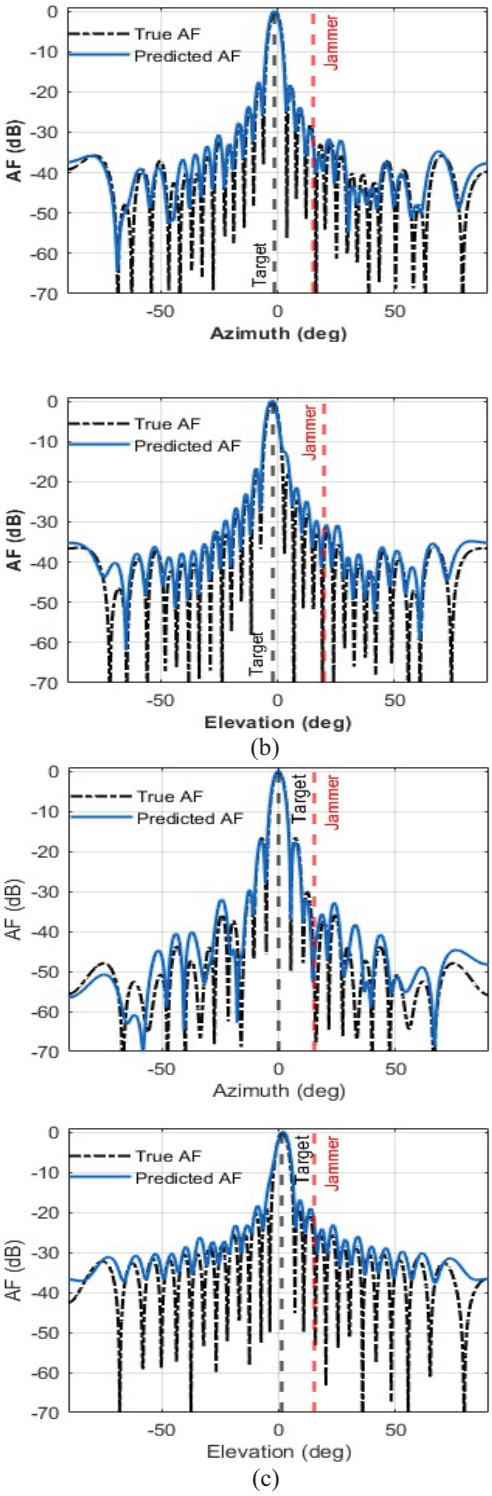

Fig. 4. 2D radiation patterns in both azimuth and elevation plans, obtained separately with true and predicted weights (deep learning) for (a) rectangular array, (b) circular array, (c) hexagonal array.

those of the MVDR reference, demonstrating that the beamwidth characteristics are well preserved.

Table 1: Summary of the comparative study results

Parameter	Notation/Description	Rectangular Array	Circular Array	Hexagonal Array
Main lobe direction (°)	$(\theta_{\max}, \phi_{\max})$	$(0,0)$	$(0,0)$	$(0,0)$
Pointing error (°)	Azimuth/Elevation	$-0.25/0.25$	$-0.25/-0.5$	$-2.5/0.5$
Side lobe level dB	SLL Az/Elev	$-14/-17.1$	$-17.8/18.5$	$-16.9/-17.6$
Jammer direction	(θ_J, ϕ_J)	$(20,15)$	$(20,15)$	$(20,15)$
Suppression level dB	SLL_J	$-30/-30.7$	$-31/-32.5$	$-30.1/-34.1$
HPBW (ϕ-plane) (°)	True	5.09	4.20	4.45
	Predicted	5.11	4.26	4.50
HPBW (θ-plane) (°)	True	3.17	4.21	4.45
	Predicted	3.26	4.22	4.77
MSE amplitude	Error	1.4×10^{-4}	4.5×10^{-4}	5.2×10^{-4}
Training time [h]	T_t (with GPU)	8:08	8:17	8:25
Running time [s]	Conventional techniques (CPU)	8.19	8.11	8.13
	CNN (CPU)	0.095	0.075	0.090
	CNN (GPU)	0.038	0.031	0.038

In terms of accuracy, the CNN achieves MSE values in the order of 10^{-4} across all array geometries, confirming the high fidelity of the predicted weights. However, more importantly, the results demonstrate that the proposed method preserves the key beamforming characteristics, including precise beam steering, effective sidelobe control, and strong interference suppression.

In addition to accuracy, the computational efficiency of the proposed approach is evaluated. To ensure a fair and consistent runtime comparison, the execution time for both the conventional MVDR method and the proposed CNN-based approach was measured under a clearly defined timing scope. For the MVDR method, the reported runtime includes the full beamforming computation process, namely covariance matrix estimation, matrix inversion, and weight computation. In contrast, for the CNN-based approach, the runtime corresponds only to the forward inference pass for predicting the beamforming weights.

All runtime measurements were conducted under identical hardware conditions to ensure a fair comparison. Results show that the CNN-based approach significantly reduces the computation time compared to the conventional MVDR method. For the rectangular array, the MVDR method requires approximately 8.19 s on a CPU, whereas the CNNbased approach requires only 0.095 s on a CPU and 0.038 s when executed on a GPU. For the circular array, the MVDR method requires 8.11 s, compared to 0.075 s (CPU) and 0.031 s (GPU) for the CNN-based approach. Similarly, for the hexagonal array, the MVDR method requires 8.13 s, while the CNN-based approach requires 0.090 s (CPU) and 0.038 s (GPU).

It is worth noting that the slight variation in runtime across different array geometries is mainly due to the difference in the number of antenna elements (640 for the rectangular array, 616 for the circular array, and 631 for the hexagonal array). However, this variation does not affect the overall conclusion, as the CNN-based approach consistently achieves a significant reduction in computation time compared to the conventional MVDR method across all configurations. These results correspond to a speed-up of approximately $90\times$ on CPU and up to $260\times$ with GPU acceleration across all array geometries.

In terms of computational complexity, the MVDR method involves matrix inversion with a complexity on the order of $O(N^3)$, where N is the number of antenna elements, whereas the CNN inference has a significantly lower computational cost dominated by convolutional operations. This substantial reduction in computational complexity explains the observed runtime improvement and highlights the suitability of the proposed approach for real-time anti-jamming applications.

V. CONCLUSION

In conclusion, this research presents a comparative study of deep learning-based beamforming techniques for anti-jamming applications utilizing 2D-planar phased arrays. By examining three distinct array geometries (circular, rectangular, hexagonal), we provide a robust framework for array architecture benchmarking. The implementation of a CNN enables the direct translation of target radiation patterns, expressed as images, into optimal antenna currents. This method efficiently estimates adaptive antenna array beam forming weights

based on specific beam steering angles and jammer null directions. Notably, our deep learning approach establishes a smart, noniterative mapping that significantly reduces computation time by up to 260 times compared to conventional optimization algorithms. Once the model is trained, it can generate optimal currents and weights swiftly in a single forward pass, demonstrating the potential of deep learning in enhancing beamforming strategies.

ACKNOWLEDGMENT

This work was funded by the Deanship of Scientific Research (DSR), King Abdulaziz University, Jeddah, Saudi Arabia, under grant No. (135-676-D1435). The authors, therefore, acknowledge with thanks DSR technical and financial support.

REFERENCES

[1] H. Hommel and H.-P. Feldle, "Current status of airborne active phased array (AESA) radar systems and future trends," in *IEEE MTT-S International Microwave Symposium Digest*, vol. 3, pp. 1449–1452, 2005.

[2] R. J. Mailloux, *Phased Array Antenna Handbook*. Norwood, MA: Artech House, 2017.

[3] E. Brookner, "Recent developments and future trends in phased arrays," in *2013 IEEE International Symposium on Phased Array Systems and Technology*, pp. 43–53, 2013.

[4] T. Kinghorn, I. Scott, and E. Totten, "Recent advances in airborne phased array radar systems," in *2016 IEEE International Symposium on Phased Array Systems and Technology (PAST)*, pp. 1–7, 2016.

[5] M. I. Skolnik, *Radar Handbook*, 3rd ed. New York, NY: McGraw-Hill, 2015.

[6] S. Maddio, G. Pelosi, M. Righini, S. Selleri, and I. Vecchi, "Optimization of the shape of non-planar electronically scanned arrays for IFF applications via multi-objective invasive weed optimization algorithm," *Applied Computational Electromagnetics Society (ACES) Journal*, vol. 35, no. 5, pp. 563–571, May 2020.

[7] R. M. Shubair, S. A. Jimaa, and A. A. Omar, "Robust adaptive beamforming using least mean mixed norm algorithm," *Applied Computational Electromagnetics Society (ACES) Journal*, vol. 23, no. 3, pp. 255–262, Sep. 2008.

[8] M. Cheng, Q. Wu, C. Yu, H. Wang, and W. Hong, "Synthesis of a thinned pre-phased electronically steered phased array using excitation control of both the small amplitude dynamic range ratio and low-resolution phase," *IEEE Transactions on Antennas and Propagation*, vol. 72, no. 1, pp. 600–613, Jan. 2024.

[9] D. Xu, Y. Zhang, H. Liu, Z. Wang, J. Chen, X. Li, Y. Wu, and K. Kang, "Ultrawideband filtering phased array antenna based on multilayer PCB and BGA-Via for AESA vertical heterogeneous integration," *IEEE Transactions on Components, Packaging and Manufacturing Technology*, vol. 15, no. 1, pp. 182–195, Jan. 2025.

[10] G. G. Khang, H.-J. Yang, Y. Lee, J. Kim, S. J. Kim, and J. Min Park, "Design results of a wideband active electrically scanned array (AESA) antenna for X-band satellite synthetic aperture radar (SAR) application," in *2024 International Symposium on Antennas and Propagation (ISAP)*, Incheon, Republic of Korea, pp. 601–602, 2024.

[11] S. Kemkemian and M. Nouvel-Fiani, "Toward common radar & EW multifunction active arrays," in *2010 IEEE International Symposium on Phased Array Systems and Technology*, Waltham, MA, USA, pp. 676–681, 2010.

[12] S. Celentano, A. Farina, L. Timmoneri, and G. Foglia, "Co-existence of (AESA) (Active Electronically Scanned Array) radar and Electronic Warfare (EW) systems on board of a military ship," in *2020 IEEE Radar Conference (RadarConf20)*, pp. 1–6, 2020.

[13] P. Sai, S. Shirsat, B. Ramkrishna, A. Bazil Raj, G. R. Shinde, and U. Sateesh, "Improvement for design of digital T/R module of X/Ka/Ku band for EW with multi-functional AESA RADAR using FPGA," in *2022 International Conference on Augmented Intelligence and Sustainable Systems (ICAISS)*, pp. 1508–1512, 2022.

[14] S. Z. M. Hamzah, N. Farihah Abdul Malek, S. Yasmin Mohamad, F. Nadia Mohd Isa, T. Surya Gunawan, and K.-S. Chin, "Deep learning-driven beam-steering for dual-polarized 28 GHz antenna arrays in 5G wireless networks," *IEEE Access*, vol. 13, pp. 80680–80694, 2025.

[15] S. Bianco, M. Feo, P. Napoletano, G. Petraglia, A. Raimondi, and P. Vinetti, "AESA adaptive beamforming using deep learning," in *Proceedings of 2020 IEEE Radar Conference*, pp. 1–6, 2020.

[16] M. Abdullah, A. Zaib, S. Khan, S. Azmat, S. Khattak, B. D. Braaten, and I. Ullah, "Antenna array pattern with sidelobe level control using deep learning," *Applied Computational Electromagnetics Society (ACES) Journal*, vol. 40, no. 5, pp. 612–620, May 2025.

[17] J. Lim, H. Yoo, E. Lee, S. Oh, and J. Lee, "Robust anti-jamming method for large-array radar systems using deep learning-based null-space beamforming," *IEEE Access*, vol. 13, pp. 103599–103612, 2025.

[18] P. Nguyen, V. Nguyen, and V. Do, "A deep double-Q learning-based scheme for anti-jamming communications," in *2020 28th European Signal Processing Conference (EUSIPCO)*, pp. 171–175, 2021.

[19] X. Liu, Y. Xu, L. Jia, Q. Wu, and A. Anpalagan, "Anti-jamming communications using spectrum waterfall: A deep reinforcement learning approach," *IEEE Communications Letters*, vol. 22, no. 5, pp. 998–1001, May 2018.

[20] G. Han, L. Xiao, and H. Poor, "Two-dimensional anti-jamming communication based on deep reinforcement learning," in *2017 IEEE International Conference on Acoustics, Speech and Signal Processing (ICASSP)*, pp. 2087–2091, 2017.

[21] C. A. Balanis, *Antenna Theory: Analysis and Design*. Hoboken, NJ: John Wiley & Sons, 2016.

[22] G. Oliveri, G. Gottardi, F. Robol, A. Polo, L. Poli, M. Salucci, M. Chuan, C. Massagrande, P. Vinetti, and M. Mattivi, "Codesign of unconventional array architectures and antenna elements for 5G base stations," *IEEE Transactions on Antennas and Propagation*, vol. 65, no. 12, pp. 6752–6767, 2017.

Aymen Alhamdan received the M.Sc. degree in electronic and electrical engineering from Strathclyde University, Glasgow, UK, in 2011. He is currently working toward the Ph.D. degree in Electronic and Computing Engineering at King Abdulaziz University, Jeddah, Saudi Arabia. His research interests are antenna array design and deep learning.

Lotfi Laadhar received his Engineering and Ph.D. degrees in Telecommunications from High Institute of Communications of Moscow, Russia, in 1985. From 1990 to 2001, he was Assistant Professor at the Air Force Academy in Tunis, Tunisia. From 2001 to 2012, he was Assistant Professor at College of Telecommunications of Jeddah. September 2012 to June 2015, he was Associate Professor at King Abdulaziz University-North Jeddah Branch College of Engineering. He became Electrical Engineering Department Chair in September 2015 and Associate Professor, King Abdelaziz University College of Engineering, Electrical Engineering Department. His research activities include wireless protocols, management of VSAT (Very Small Aperture Terminal) services such as IP connect and IP access, including internet through the satellite (one-way and the 2-way), in addition to antennas and metasurfaces.

Mohammed Aseeri is currently Full Professor at King Abdulaziz City for Science and Technology (KACST), Saudi Arabia, working within the National Center for Radar and Electronic Technology, and serves as Co-Principal Investigator at the Center of Excellence for Microwave Sensor Technology (CMST), a joint initiative between KACST and the University of Michigan, USA. He received his Bachelor's and M.Sc. degrees in Electrical and Computer Engineering (Electronics and Communications) from King Abdulaziz University, and his Ph.D. in Electronics from the University of Kent, Canterbury, UK. He is a certified Consultant Engineer by the Saudi Council of Engineers (SCE) and holds a Project Management Professional (PMP) certification from PMI. He has gained international research experience through his work as a researcher at the Australian National University (ANU) and the University of Canberra (UC). His professional experience includes managing and supervising advanced electronic surveillance systems and leading multiple national-level projects. His research interests focus on radar systems, electronic warfare, signal processing, wireless sensor networks (WSN), and AI-integrated intelligent sensing systems, including anti-jamming techniques and advanced beamforming for phased array antennas. He is also actively engaged in innovation, technology localization, and the development of smart IoT-based solutions for environmental monitoring and infrastructure protection. He is a senior member of IEEE and IET and has authored numerous scientific publications in highimpact journals and international conferences. He also holds several patents and contributes actively to advancing research, innovation, and strategic technology development.

Abdullah Dobaie received his B.Sc. in 1981 and M.Sc. in 1989, both in Electronic and Communication Engineering from King Abdulaziz University in Saudi Arabia, and Ph.D. in 1995 from Colorado State University, USA. He has supervised many masters and doctoral students in electrical and communication area and has directed many projects concerning communication, digital filters, antenna, and digital signal processing. His recent interests include adaptive communication systems, digital image processing, wave propagation, and communication networks.

Hatem Rmili (Senior Member, IEEE) received the B.S. degree in physics from the Science Faculty of Monastir, Tunisia, in 1995, and the DEA diploma (Master) from the Science Faculty of Tunis, in quantum mechanics, in 1999. He received the Ph.D. degree in physics (electronics) from the University of Bordeaux 1, France, in 2004. From December 2004 to March 2005, he was a research assistant in the PIOM laboratory at the University of Bordeaux 1. From March 2005 to March 2007, he was a Postdoctoral Fellow at the Rennes Institute of Electronics and Telecommunications. From March to September 2007, he was a Postdoctoral Fellow at the ESEO engineering school, in Angers. From September 2007 to August 2012, he was an assistant professor with the Mahdia Institute of Applied Science and Technology (ISSAT), Department of Electronics and Telecommunications, Tunisia. He was an Assistant/Associate/Full Professor (from 2012 to 2024) with the Electrical and Computer Engineering Department, Faculty of Engineering, King Abdulaziz University, Jeddah, Saudi Arabia. In March 2024, Rmili joined Prince Sultan Defense Studies and Research Center (PSDSARC), Riyadh, as Radar Systems Expert. Rimli's research interests concern applied electromagnetic applications involving radar, antennas, AESA, metamaterials, and metasurfaces. The main targeted applications are reconfigurable antennas for multi-standard wireless communications systems, security of chipless RFID systems with fractal tags, terahertz photoconductive antennas for infra-red energy harvesting, UWB nano rectennas for collection of solar energy, phase shifters for low-cost 5G communication systems, radar beamforming, high power microwave, and microwave absorbing materials for stealth technologies.